Inorganic Chemistry
Article
pubs.acs.org/IC

Observing the Transition from Equatorial to Axial CO Chemisorption: Infrared Photodissociation Spectroscopy of Yttrium Oxide−Carbonyls

Hua Xie,[†,§] Zhiling Liu,[‡,§] Zhi Zhao,[†] Xiangtao Kong,[†] Hongjun Fan,[†] Zichao Tang,[*,†] and Ling Jiang[*,†]

[†]State Key Laboratory of Molecular Reaction Dynamics, Collaborative Innovation Center of Chemistry for Energy and Materials (iChEM), Dalian Institute of Chemical Physics, Chinese Academy of Sciences, 457 Zhongshan Road, Dalian 116023, Liaoning, P. R. China

[‡]School of Chemistry and Material Science, Shanxi Normal University, Linfen 041004, Shanxi, P. R. China

S Supporting Information

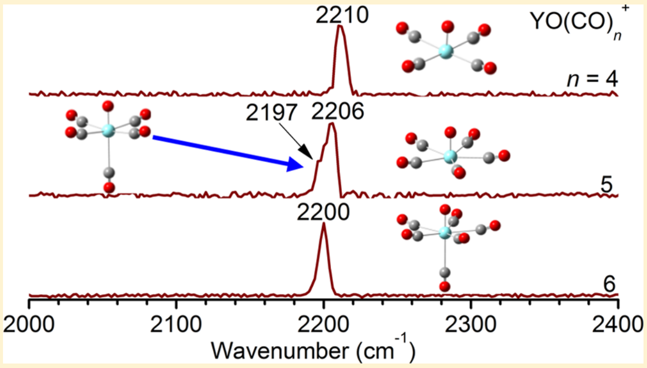

ABSTRACT: A series of yttrium oxide−carbonyls are prepared via a laser vaporization supersonic cluster source in the gas phase and identified by mass-selected infrared photodissociation (IRPD) spectroscopy in the C−O stretching region and by comparing the observed IR spectra with those from quantum chemical calculations. For $YO(CO)_4^+$, all four CO ligands prefer to occupy the equatorial site of the YO^+ unit, leading to a quadrangular pyramid with C_{4v} symmetry. Two energetically nearly degenerate isomers are responsible for $YO(CO)_5^+$, in which the fifth CO ligand is either inserted into the equatorial plane of $YO(CO)_4^+$ or coordinated opposite the oxygen on the C_4 axis. $YO(CO)_6^+$ has a pentagonal bipyramidal structure with C_{5v} symmetry, which includes five equatorial CO ligands and one axial CO ligand. The present IRPD spectroscopic and theoretical study of $YO(CO)_n^+$ extends the first shell coordination number of CO ligands in metal monoxide carbonyls to six. The transition from equatorial to axial CO chemisorption in these yttrium oxide−carbonyls is fortunately observed at $n = 5$, providing new insight into ligand interactions and coordination for the transition metal oxides.

1. INTRODUCTION

Transition metal oxides have been widely studied due to their important roles in many applications, such as catalysis, electronics, chemical sensors, and medicine.[1−6] Extensive efforts have been made to address the interaction of a series of inorganic or organic molecules with metal oxides.[7−10] In particular, carbon monoxide is employed as the reagent in many industrial processes (i.e., Fischer−Tropsch synthesis and hydroformylation), which has motivated numerous experimental and theoretical investigations of CO chemisorption on transition metal oxide surfaces. The study on the coordination nature of carbon monoxide with metal oxide cluster is of considerable interest, because it serves as the prototypical model system for fundamentally understanding the multifaceted mechanisms of carbon monoxide activation by metal oxide clusters and surfaces.

The 18-electron rule is often used to predict the relative stabilities and coordination numbers of transition metal carbonyls. The series $Ni(CO)_4 \rightarrow Fe(CO)_5 \rightarrow Cr(CO)_6$ represents well-known 18-electron neutral carbonyls. Recent studies have demonstrated that the infrared photodissociation (IRPD) spectroscopy combined with theoretical calculation is one of the most powerful and generally applicable techniques for structural characterization of metal clusters and their carbonyl ions.[11−21] With these methods, niobium and tantalum have been found to form seven-coordinate carbonyls, $Nb(CO)_7^+$ and $Ta(CO)_7^+$, which have C_{3v} capped octahedral structures.[14] Significant progress has been made by the successful identification of homoleptic carbonyls of $U(CO)_8^+$ and $Y(CO)_8^+$,[15,20] extending the coordination number known for metal carbonyls to eight.

In contrast with extensive explorations of metal carbonyls, much less work has been done for metal oxide carbonyls. A few transition metal monoxide carbonyl complexes, $OMCO^{+/0/-}$ (M = Sc−Cu), have been isolated in a solid argon matrix and characterized using matrix-isolation infrared spectroscopy.[22−27] Gas-phase studies have shown that the coordination number of CO in $MO(CO)_6^+$ (M = V, Ti) is five, which allows structures to be built by the weak attachment of "external" CO ligand onto the $MO(CO)_5^+$ core ion.[17,18] Here, we report a study on the structural evolution of yttrium oxide−carbonyl complexes, $YO(CO)_n^+$. IRPD spectra and theoretical calculations reveal that YO^+ could coordinate at least six CO ligands in the first

Received: March 1, 2016
Published: May 9, 2016

DOI: 10.1021/acs.inorgchem.6b00519

sphere, and the transition from equatorial to axial CO chemisorption in the yttrium oxide−carbonyls occurs at $n = 5$.

2. EXPERIMENTAL METHOD

The experiments have been carried out using a homemade infrared photodissociation apparatus, including a laser vaporization supersonic cluster source, a tandem TOF mass spectrometer, and a tunable infrared laser source.[28] The experimental setup has been previously described in detail. Briefly, a 532 nm laser beam from a Nd: YAG laser is focused to vaporize the rotating metal targets. The purities of the targets are better than 99.9%. The $YO(CO)_n^+$ complexes are produced by the reactions of the vaporized species with 2% O_2 seeded in CO. The stagnation pressure of the reaction gas is approximately 8−10 atm, and the gas is introduced into a vacuum region using a pulsed valve. After the free expansion, the cationic complexes are skimmed into the acceleration region and analyzed using the first stage of the TOF system. The cations of interest are mass-selected and decelerated into the extraction region of a vertical second stage of the TOF system. Here, they interact with the IR laser pulse from a Laservision OPO/OPA IR laser. The dissociation fragments and the remaining parent cations are analyzed using the vertical second stage of the TOF mass spectrometer. Typical spectra are recorded by scanning the infrared laser in steps of 2 cm^{-1} and averaging approximately 300 laser shots at each wavelength.

The tunable infrared laser beam is generated by a KTP/KTA optical parametric oscillator/amplifier system (OPO/OPA, LaserVision) pumped by an injection-seeded Continuum Surelite Nd:YAG laser. This system is tunable from 700 to 7000 cm^{-1} with a line width of 1 cm^{-1}. The infrared laser beam is loosely focused using a CaF_2 convex lens before entering the infrared photodissociation region. The wavelength of the OPO laser output is calibrated using a commercial wavelength meter (Bristol, 821 Pulse Laser Wavelength Meter).

3. COMPUTATIONAL METHODS

Quantum chemical calculations are performed using the Gaussian 09 program.[29] Recent investigations have demonstrated that the B3LYP hybrid functional can well reproduce the infrared photodissociation spectroscopic experiments of scandium and yttrium carbonyl cations.[20] Therefore, this functional is employed for the present calculations as well. The DZP basis set is used for carbon and oxygen atoms,[30] and the LanL2DZ ECP basis set is used for yttrium.[31,32] Relative energies and binding energies include zero-point vibrational energies. Carbonyl stretching frequencies are scaled by a factor of 0.971,[20,33,34] which is derived by comparing the frequencies computed at this same level of theory for $Cr(CO)_6$, $Fe(CO)_5$, and $Ni(CO)_4$ to their known experimental values. The resulting stick spectra are convoluted by a Gaussian line shape function with a width of 8 cm^{-1} (fwhm).

4. RESULTS AND DISCUSSION

Laser vaporization of metal rods with 2% O_2 seeded in CO produces the $YO(CO)_n^+$ ($n = 4−6$) complexes. The mass spectrum is given in Figure S1 in the Supporting Information. These metal species of interest are mass-selected and introduced into the infrared photodissociation region. The selected cations can absorb photons and fragment by losing CO(s) when the IR-active vibration of the cation is resonant with the tunable infrared laser frequency. Infrared photodissociation spectra are acquired by recording the fragment ions as a function of the wavelength of tunable infrared laser.

4.1. Experimental Infrared Photodissociation Spectra.

The $YO(CO)_n^+$ complexes are observed to dissociate via losing one CO molecule with low efficiency under the focused infrared laser beam. All the cations are depleted by less than 5% when the infrared laser energy is approximately 1 mJ/pulse around 2200 cm^{-1}. Dissociation energy for the loss of one CO in $OYCO^+$ was measured to be 68.5 kJ/mol,[35] indicating that, assuming internally cold complexes, the absorption of at least three photons around 2200 cm^{-1} is required to overcome the dissociation limit. The intense and tunable infrared radiation source (i.e., Infrared free electron laser) is needed to achieve efficient multiphoton dissociation of strongly bound complexes. Alternatively, the technique of "messenger tagging" could be used to enhance the dissociation yield.[11,12,19,36−40] Under the appropriate conditions (i.e., efficient cooling by supersonic expansion or cryogenic ion trap), the tagged complexes could be formed with weakly attached inert species that are transparent in the infrared (i.e., H_2, rare gas atoms), which are readily dissociated upon absorption of a single IR photon resonant because of low binding energy of "the messenger". Unfortunately, it is difficult to generate sufficient tagged-$YO(CO)_n^+$ complexes for the photodissociation measurement, which might be due to the warm source under the present experimental conditions. The IRPD spectra of $YO(CO)_n^+$ ($n = 4−6$) are successfully measured in the C−O stretching region using the table-top LaserVision system, which are shown in Figure 1. The Y−O stretch vibration in these clusters is absent because of the weak infrared laser from the table-top LaserVision system in this region and low tagging efficiency.

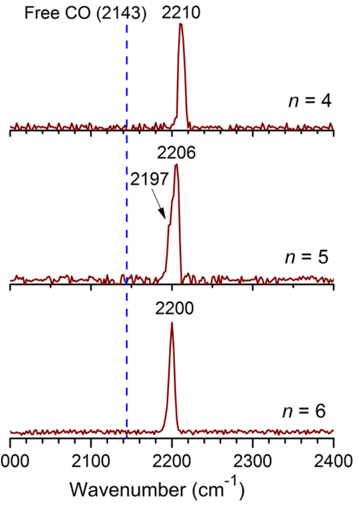

Figure 1. Experimental IRPD spectra of the $YO(CO)_n^+$ ($n = 4−6$) complexes. The CO stretch in the free CO molecule (2143 cm^{-1}) is indicated with a dashed vertical blue line.

Vibrational frequency in the $YO(CO)_n^+$ ($n = 4−6$) complexes is observed around 2210, 2206, and 2200 cm^{-1}, respectively, which is blue-shifted by 67, 63, and 57 cm^{-1} from the free CO molecule (2143 cm^{-1}). These band positions of CO stretches in $YO(CO)_n^+$ ($n = 4−6$) are characteristic of terminal carbonyl ligands and nonclassical carbonyls.[41] Interestingly, a shoulder peak is observed at 2197 cm^{-1} in the IRPD spectrum of $YO(CO)_5^+$, resulting in a broader band width than $YO(CO)_4^+$ and $YO(CO)_6^+$. The fwhm of bands in the IRPD spectrum for $YO(CO)_5^+$ (14 cm^{-1}) is observably larger than that for $YO(CO)_4^+$ (9 cm^{-1}) and $YO(CO)_6^+$ (7 cm^{-1}), indicating that the shoulder peak in the IRPD spectrum of $YO(CO)_5^+$ could be real.

4.2. Optimized Structures.

Optimized structures of the minimum-energy isomers of the $YO(CO)_n^+$ ($n = 4−6$) complexes are illustrated in Figure 2. For the $n = 4$ cluster, the lowest-lying structure is predicted to be square pyramidal with C_{4v} symmetry and the $^1A_1$ state (**4A**), in which the four

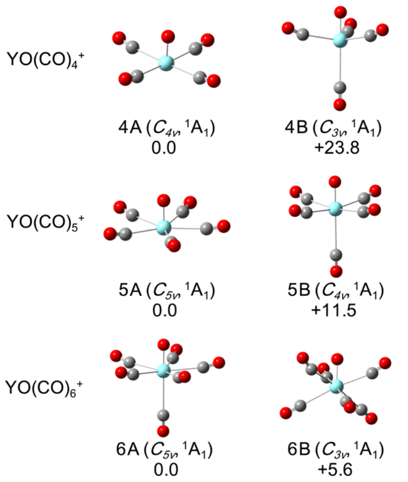

Figure 2. Optimized structures of the minimum-energy isomers of the $YO(CO)_n^+$ (n = 4−6) complexes. Relative energies (with ZPE correction) are given in kJ/mol.

CO ligands are equally coordinated to the Y center in the equatorial plane. The **4B** isomer lies 23.8 kJ/mol higher in energy above **4A** and consists of a trigonal bipyramidal structure with C_{3v} symmetry, in which three CO ligands are equatorially bonded to the Y atom and one CO is coordinated opposite the oxygen on the C_3 axis. In the lowest-energy isomer for the n = 5 cluster, **5A**, the five CO ligands are in the equatorial plane, as shown in Figure 2. Each CO is terminally coordinated to the Y atom, resulting in a pentagonal pyramidal structure with C_{5v} symmetry. The next energetically higher isomer, **5B**, lies 11.5 kJ/mol above **5A** and has four terminal CO ligands in the equatorial plane and one CO on the C_4 axis. For n = 6, the lowest-energy isomer (**6A**) is predicted to have a pentagonal bipyramidal structure with C_{5v} symmetry, which includes five equatorial carbonyl ligands and one axial carbonyl ligand (Figure 2). The **6B** isomer has a monocapped antitriangular prism conformation with C_{3v} symmetry, which lies 5.6 kJ/mol above **6A**.

4.3. Comparison of Infrared Photodissociation Spectra with Theoretical Calculations.

Experimental IRPD spectra and simulated harmonic vibrational spectra of the $YO(CO)_n^+$ (n = 4−6) complexes are compared in Figure 3. In the n = 4 cluster, only one intense and sharp band is experimentally observed in the carbonyl stretching region, resulting in four equivalent CO ligands. As illustrated in Figure 3, carbonyl stretching frequencies in the **4A** isomer are predicted to be 2200 cm^{-1}, which is in excellent agreement with the experimental value of 2210 cm^{-1}. The simulated carbonyl stretching frequencies in the **4B** isomer are 2186 and 2197 cm^{-1}, yielding a broader band than **4A**, which is observably different from the experiment. Then, the contribution of the **4B** isomer to $YO(CO)_4^+$ can be ruled out. In the simulated harmonic vibrational spectra of $YO(CO)_5^+$, the **5A** isomer exhibits one single band at 2192 cm^{-1} and the **5B** isomer gives one intense band at 2195 cm^{-1} with a shoulder peak at 2182 cm^{-1}, in which band positions agree with the experiment. Therefore, the coexistence of the **5A** and **5B** isomers is likely here. In the **6A** isomer for $YO(CO)_6^+$, one single band is predicted at 2187 cm^{-1}, which well reproduces the experimental feature. In contrast, two bands are observed at 2166 and 2190 cm^{-1} in the **6B** isomer, which is remarkably different from the experiment. Note that the relative energy for **5A** and **5B** (11.5 kJ/mol) is larger than that for **6A** and **6B** (5.6 kJ/mol). The lowest binding energy of one CO molecule for the **5A**, **5B**, **6A**, and **6B** isomers is calculated to be 45.9, 34.4, 33.9, and 28.4 kJ/mol (Table S1), respectively. Considering that the association and dissociation of the cluster are competitive under given conditions, the presence of the two isomers for $YO(CO)_5^+$ (**5A** and **5B**) and only one isomer for $YO(CO)_6^+$ (**6A**) implies that the association of **6B** is unfavorable in the warm source under the current experimental conditions because of its low binding energy.

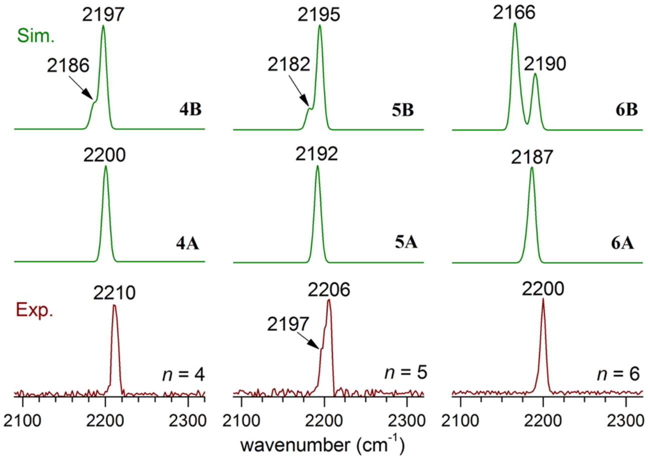

Figure 3. Experimental IRPD spectra (in red) and simulated harmonic vibrational spectra (in green) of the $YO(CO)_n^+$ (n = 4−6) complexes.

4.4. Structural Evolution and Bonding Mechanism of $YO(CO)_n^+$ Complexes.

The agreement between the experimental spectra and those that are simulated is achieved from the aforementioned analysis, which is helpful for the structural assignment of $YO(CO)_n^+$ (n = 4−6). For the minimum-energy structure of $YO(CO)_4^+$, the quadrangular pyramid of C_{4v} symmetry with all four equivalent end-on bonded CO ligands (**4A**) is favored, which is analogous to $TiO(N_2)_4$.[42] Two low-lying isomers of **5A** and **5B** are found to be responsible for $YO(CO)_5^+$, which could be viewed as being built from $YO(CO)_4^+$ by insertion of an additional CO into the equatorial plane of $YO(CO)_4^+$ or axially adsorbing an additional carbonyl group. The configuration of the **5A** isomer is reminiscent of $ScO(Ng)_5^+$ (Ng = Ar, Kr, and Xe), $YO(Xe)_5^+$, $TiO(CO)_5^+$, and $VO(CO)_5^+$.[17,18,43,44] The **6A** isomer is assigned to be the structure of $YO(CO)_6^+$, which is derived from the **5A** structure of $YO(CO)_5^+$ by axially adsorbing an additional carbonyl group. This is similar to $YO(Ar)_6^+$ and $YO(Kr)_6^+$.[43]

The weak depletion and fragment production in the region of the carbonyl stretch indicate that all the CO ligands should chemically coordinate to the YO^+ unit. During the sequential carbonylation process, the first three carbonyl groups are predicted to successively surround the yttrium center of the YO^+ core in the quasi-perpendicular direction and construct umbrella-like structure, as shown in Figure S1 (Supporting Information). The fourth carbonyl ligand continuously inserts into the equatorial plane to form a quadrangular pyramidal structure. The first four carbonyl groups are apparently rib-like ligands. For $YO(CO)_5^+$, two energetically degenerate isomers are experimentally confirmed. As compared to $YO(CO)_4^+$, the fifth carbonyl ligand in $YO(CO)_5^+$ attaches either equatorially to the yttrium atom to form an umbrella-like pentagonal pyramid or opposite the oxygen on the C_4 axis to form a top-shaped quadrangular bipyramid. The sixth carbonyl ligand is axially bonded to the umbrella-shaped isomer of $YO(CO)_5^+$ to form a top-shaped pentagonal bipyramid. Thus, it can be concluded that during the sequential carbonylation process of $YO(CO)_n^+$ ($n = 4-6$), the $YO(CO)_n^+$ system prefers to adopt an umbrella-shaped structure so that the terminal carbonyl ligands preferentially occupy the equatorial site of the YO^+ unit, and then an additional carbonyl group is axially bonded to the YO^+ unit to form the top-shaped structure. The umbrella-shaped to top-shaped structural evolution in the $YO(CO)_n^+$ complexes suggests that the equatorial-to-axial chemisorbed transition occurs at $n = 5$.

Interestingly, the IR spectra of $VO(CO)_n^+$ and $TiO(CO)_n^+$ ($n = 5-6$) exhibit a single intense band in the carbonyl stretch region along with one or two weaker bands on the higher energy side,[17,18] which is different from those of $YO(CO)_n^+$ ($n = 5-6$). Such a spectral difference implies the structural diversity among these metal oxide–carbonyl complexes. Recent studies have indicated that, in the $VO(CO)_n^+$ and $TiO(CO)_n^+$ complexes, the maximum number of chemisorbed CO ligands is five, and the remaining "external" carbonyl groups are physisorbed in the second sphere via weak electronic interactions.[17,18] In this work, the first shell coordination number of CO ligands in $YO(CO)_n^+$ is six, which is larger than that of the VO^+ and TiO^+ unit. In contrast, the YO^+ cation was found to coordinate six Ar or Kr atoms, and five Xe atoms in solid noble gas matrixes.[43] The neutral YO unit consists of a $^2\Sigma$ ground state with an electron configuration of $(\text{core})(\sigma)^1$. Since this σ orbital is singly occupied, the coordination in the axial direction is weak due to σ repulsion. While the YO^+ cation is formed with the $^1\Sigma$ ground state, this σ repulsion is reduced upon removing this σ electron. Consequently, the fifth CO is able to coordinate to YO^+ in the axial direction. This bonding feature is manifested by the pictures for the lowest unoccupied molecular orbitals (LUMOs) and highest occupied molecular orbitals (HOMOs) of the isomers (Figure 4), in which the LUMOs consist of π orbitals localized on the interaction of CO ligands with the Y center and the HOMOs are mainly nonbonding for CO ligands.

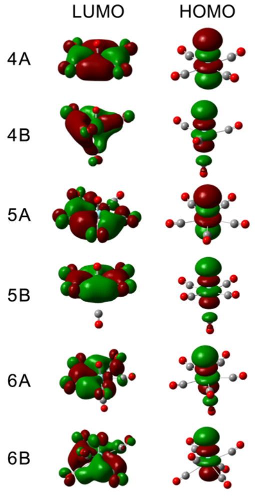

Figure 4. LUMO and HOMO pictures for the isomers of $YO(CO)_n^+$ ($n = 4-6$).

5. CONCLUSIONS

The approach of infrared photodissociation spectroscopy combined with quantum chemical calculation is employed to probe the structural evolution of gaseous yttrium oxide–carbonyls. The $YO(CO)_n^+$ cations are generated via a laser vaporization supersonic cluster source in the gas phase and mass selected to interact with the infrared laser in the carbonyl stretching region. The agreement between experiment and theory is achieved, which demonstrates that the terminally bonded carbonyl groups preferentially occupy the equatorial site of the YO^+ unit to construct the umbrella-shaped structure, and the equatorial-to-axial chemisorbed transition in the $YO(CO)_n^+$ complexes occurs at $n = 5$. The optimum coordinated number of CO ligands around the YO^+ cation is found to be six, which is larger than that of VO^+ and TiO^+ cations reported previously.[17,18] This finding extends the range of coordination numbers of CO ligands in metal-oxide carbonyls and provides new insight into the ligand interactions and coordination properties of transition metal oxides with small molecules.

■ ASSOCIATED CONTENT

Ⓢ Supporting Information

The Supporting Information is available free of charge on the ACS Publications website at DOI: 10.1021/acs.inorg-chem.6b00519.

> Mass spectrum of the ions (Figure S1); optimized structures of $YO(CO)_n^+$ ($n = 1-8$) (Figure S2); Cartesian coordinates, energies, and unscaled harmonic frequencies of the isomers (PDF)

■ AUTHOR INFORMATION

Corresponding Authors

*E-mail: ljiang@dicp.ac.cn (L.J.).
*E-mail: zctang@dicp.ac.cn (Z.T.).

Author Contributions

§H.X. and Z.L.L. contributed equally.

Notes

The authors declare no competing financial interest.

■ ACKNOWLEDGMENTS

This work was supported by the National Natural Science Foundation of China (Grant No. 21273233, 21327901, 21321091, and 21503222), the Ministry of Science and Technology of China (Grant No. 2011YQ09000505). L.J. acknowledges the Hundred Talents Program of Chinese Academy of Sciences.

■ REFERENCES

(1) Cox, P. A. *Transition Metal Oxides*; Clarendon: Oxford, U.K., 1992.
(2) Campbell, C. T. *Surf. Sci. Rep.* **1997**, *27*, 1−111.
(3) Rao, C. N.; Raveau, B. *Transition Metal Oxides*; Wiley: New York, 1998.
(4) Luo, X. L.; Morrin, A.; Killard, A. J.; Smyth, M. R. *Electroanalysis* **2006**, *18*, 319−326.
(5) Hill, C. L. *J. Mol. Catal. A: Chem.* **2007**, *262*, 2−6.
(6) Gong, Y.; Zhou, M.; Andrews, L. *Chem. Rev.* **2009**, *109*, 6765−6808.
(7) Huheey, J. E.; Keiter, R. L.; Keiter, E. A. *Inorganic Chemistry Principles of Structure and Reactivity*; Harper Collins: New York, 1993.

(8) Somorjai, G. A. *Introduction to Surface Chemistry and Catalysis*; Wiley: New York, 1994.

(9) Cotton, F. A.; Wilkinson, G.; Murillo, C. A.; Bochmann, M. *Advanced Inorganic Chemistry*, 6th ed.; John Wiley & Sons: New York, 1999.

(10) Hartwig, J. F. *Organotransition Metal Chemistry*; University Science Books: Sausalito, CA, 2000.

(11) Duncan, M. A. *Int. Rev. Phys. Chem.* **2003**, *22*, 407−435.

(12) Walker, N. R.; Walters, R. S.; Duncan, M. A. *New J. Chem.* **2005**, *29*, 1495−1503.

(13) Gruene, P.; Rayner, D. M.; Redlich, B.; van der Meer, A. F. G.; Lyon, J. T.; Meijer, G.; Fielicke, A. *Science* **2008**, *321*, 674−676.

(14) Ricks, A. M.; Reed, Z. D.; Duncan, M. A. *J. Am. Chem. Soc.* **2009**, *131*, 9176−9177.

(15) Ricks, A. M.; Gagliardi, L.; Duncan, M. A. *J. Am. Chem. Soc.* **2010**, *132*, 15905−15907.

(16) Asmis, K. R. *Phys. Chem. Chem. Phys.* **2012**, *14*, 9270−9281.

(17) Zhou, X.; Cui, J.; Li, Z. H.; Wang, G.; Liu, Z.; Zhou, M. *J. Phys. Chem. A* **2013**, *117*, 1514−1521.

(18) Brathwaite, A. D.; Ricks, A. M.; Duncan, M. A. *J. Phys. Chem. A* **2013**, *117*, 13435−13442.

(19) Wang, G.; Zhou, M.; Goettel, J. T.; Schrobilgen, G. J.; Su, J.; Li, J.; Schloeder, T.; Riedel, S. *Nature* **2014**, *514*, 475−478.

(20) Brathwaite, A. D.; Maner, J. A.; Duncan, M. A. *Inorg. Chem.* **2014**, *53*, 1166−1169.

(21) Xie, H.; Liu, Z.; Xing, X.; Tang, Z. *Chem. Phys. Lett.* **2015**, *628*, 66−70.

(22) Chertihin, G. V.; Andrews, L. *J. Am. Chem. Soc.* **1995**, *117*, 1595−1602.

(23) Zhou, M.; Andrews, L. *J. Am. Chem. Soc.* **1998**, *120*, 13230−13239.

(24) Zhou, M.; Andrews, L. *J. Phys. Chem. A* **1999**, *103*, 2066−2075.

(25) Zhou, M.; Liang, B.; Andrews, L. *J. Phys. Chem. A* **1999**, *103*, 2013−2023.

(26) Liang, B.; Andrews, L. *J. Phys. Chem. A* **2002**, *106*, 595−602.

(27) Liang, B.; Andrews, L. *J. Phys. Chem. A* **2002**, *106*, 4042−4053.

(28) Xie, H.; Wang, J.; Qin, Z.; Shi, L.; Tang, Z.; Xing, X. *J. Phys. Chem. A* **2014**, *118*, 9380−9385.

(29) Frisch, M. J.; Trucks, G. W.; Schlegel, H. B.; Scuseria, G. E.; Robb, M. A.; Cheeseman, J. R.; Scalmani, G.; Barone, V.; Mennucci, B.; Petersson, G. A.; Nakatsuji, H.; Caricato, M.; Li, X.; Hratchian, H. P.; Izmaylov, A. F.; Bloino, J.; Zheng, G.; Sonnenberg, J. L.; Hada, M.; Ehara, M.; Toyota, K.; Fukuda, R.; Hasegawa, J.; Ishida, M.; Nakajima, T.; Honda, Y.; Kitao, O.; Nakai, H.; Vreven, T.; Montgomery, J. A.; Peralta, J. E.; Ogliaro, F.; Bearpark, M.; Heyd, J. J.; Brothers, E.; Kudin, K. N.; Staroverov, V. N.; Kobayashi, R.; Normand, J.; Raghavachari, K.; Rendell, A.; Burant, J. C.; Iyengar, S. S.; Tomasi, J.; Cossi, M.; Rega, N.; Millam, J. M.; Klene, M.; Knox, J. E.; Cross, J. B.; Bakken, V.; Adamo, C.; Jaramillo, J.; Gomperts, R.; Stratmann, R. E.; Yazyev, O.; Austin, A. J.; Cammi, R.; Pomelli, C.; Ochterski, J. W.; Martin, R. L.; Morokuma, K.; Zakrzewski, V. G.; Voth, G. A.; Salvador, P.; Dannenberg, J. J.; Dapprich, S.; Daniels, A. D.; Farkas; Foresman, J. B.; Ortiz, J. V.; Cioslowski, J.; Fox, D. J. *Gaussian 09*, revision A.02.; Wallingford, CT, 2009.

(30) Dunning, T. H. *J. Chem. Phys.* **1970**, *53*, 2823−2833.

(31) Krishnan, R.; Binkley, J. S.; Seeger, R.; Pople, J. A. *J. Chem. Phys.* **1980**, *72*, 650−654.

(32) McLean, A. D.; Chandler, G. S. *J. Chem. Phys.* **1980**, *72*, 5639−5648.

(33) Ricks, A. M.; Reed, Z. E.; Duncan, M. A. *J. Mol. Spectrosc.* **2011**, *266*, 63−74.

(34) Brathwaite, A. D.; Duncan, M. A. *J. Phys. Chem. A* **2013**, *117*, 11695−11703.

(35) Sievers, M. R.; Armentrout, P. B. *Inorg. Chem.* **1999**, *38*, 397−402.

(36) Okumura, M.; Yeh, L. I.; Lee, Y. T. *J. Chem. Phys.* **1985**, *83*, 3705−3706.

(37) Okumura, M.; Yeh, L. I.; Lee, Y. T. *J. Chem. Phys.* **1988**, *88*, 79−91.

(38) Ayotte, P.; Weddle, G. H.; Kim, J.; Johnson, M. A. *J. Am. Chem. Soc.* **1998**, *120*, 12361−12362.

(39) Hamashima, T.; Li, Y.-C.; Wu, M. C. H.; Mizuse, K.; Kobayashi, T.; Fujii, A.; Kuo, J.-L. *J. Phys. Chem. A* **2013**, *117*, 101−107.

(40) Heine, N.; Asmis, K. R. *Int. Rev. Phys. Chem.* **2015**, *34*, 1−34.

(41) Lupinetti, A. J.; Frenking, G.; Strauss, S. H. *Angew. Chem., Int. Ed.* **1998**, *37*, 2113−2116.

(42) Zhou, M.; Zhuang, J.; Zhou, Z.; Li, Z. H.; Zhao, Y.; Zheng, X.; Fan, K. *J. Phys. Chem. A* **2011**, *115*, 6551−6558.

(43) Zhao, Y.; Gong, Y.; Chen, M.; Ding, C.; Zhou, M. *J. Phys. Chem. A* **2005**, *109*, 11765−11770.

(44) Zhao, Y.; Wang, G.; Chen, M.; Zhou, M. *J. Phys. Chem. A* **2005**, *109*, 6621−6623.